Electronic Supplementary Information

NiFeCe nanosheet arrays by N and P doping as efficient electrocatalysts for oxygen evolution reaction

Chao Xu[a], Qiangqiang Wang[a], Xuan Kuang[a], Xu Sun[a], Xiang Ren[a], Dan Wu[a*], Qin Wei[a,b*]

a School of Chemistry and Chemical Engineering, University of Jinan, Jinan 250022, Shandong, China.

b Department of Chemistry, Sungkyunkwan University, Suwon, 16419, Republic of Korea.

*Corresponding authors: Dan Wu, Qin Wei

E-mail: wudan791108@163.com (D. Wu); sdjndxwq@163.com (Q. Wei)

Additional Experimental Details

Materials and chemicals

All chemicals involved in the experiment are analytical grade and require no further purification. $NiCl_2·6H_2O$, $FeCl_2$, CH_4N_2O, $Ce(NO_3)_3·6H_2O$, $NaH_2PO_2·H_2O$, NH_4HCO_3 were bought from Macklin. Nickel foams (NF, areal density 280 g/m^2 , 0.5 mm thick) were purchased from Suzhou Kesheng Experimental Equipment Co., LTD. Pt/C (20 wt% Pt on Vulcan XC-72R) were purchased from Jinan Jiadong Chemical Co., LTD. The ultrapure water (UP H_2O) was obtained using the AD3L-05-030OR UP H_2O instrument.

Materials characterization

X-ray diffraction (XRD) patterns were recorded on a Rigaku D/MAX 2550 diffractometer utilizing Cu Kα radiation (λ = 1.5418 Å) over a 2θ range of 5° to 80°. Scanning electron microscopy (SEM) analysis was conducted using an FEI XL30 ESEM FEG microscope operating at an accelerating voltage of 20 kV and the energy dispersive X-ray detector (EDX) was characterized using JeOLJSM-6700F. Transmission electron microscopy (TEM) and high-resolution TEM (HRTEM) data were acquired on a JEOL JEM 2100 microscope at an accelerating voltage of 200 kV. X-ray photoelectron spectroscopy (XPS) measurements were carried out on a Thermo Fisher Scientific ESCALAB 250 spectrometer, with the C 1s peak (binding energy = 284.8 eV) serving as the reference for charge correction. The brunauer-emmett-teller (BET) surface area measurements were determined via N_2 adsorption using a Micromeritics ASAP 2460 analyzer.

Electrochemical measurements

All electrochemical data were obtained by an electrochemical workstation under room temperature of 26 ℃ and alkaline conditions. A three-electrode system consisting of graphite electrode as counter electrode, Hg/HgO as reference electrode, synthesized material (0.25 cm^2) as working electrode, and 1.0 M KOH as electrolyte was used to measure the OER catalytic performance of a series of samples. The oxygen evolution reaction (OER) electrocatalytic activity of the N-$Ni_{0.75}Fe_{0.15}Ce_{0.10}$P/NF composite was characterized via linear sweep voltammetry (LSV) at a scan rate of 1 mV s^{-1}

Convert all potential data into reversible hydrogen electrodes (RHE) using Equation 3-1:

$$E_{RHE} = E_{Hg/HgO} + 0.197\ V + 0.0591 \times pH - i \times R_s \quad (3\text{-}1)$$

Where R_s is the impedance (Ω), and i is the current (A).

Convert the polarization curve into a Tafel slope using Equation 3-2:

$$\eta = a + b \times \log j \quad (3\text{-}2)$$

Where η is the overpotential, b is the Tafel slope, and j is the current density.

Evaluate the electrochemical active surface area (ECSA) using Equation 3-3:

$$i_p = 0.4463 \times 10^{-3} \times n^{3/2} \times F^{3/2} \times A \times C_{R*} \times D_R^{1/2} \times v^{1/2} \times (RT)^{-1/2} \quad (3\text{-}3)$$

Where n is the number of transferred electrons (potassium ferricyanide, $n = 1$), F is Faraday constant (96485 C mol^{-1}), R is the gas constant (8.314 J mol^{-1} K^{-1}), T is the temperature (298 K), C_{R*} (mol L^{-1}) is the concentration of potassium ferricyanide, v is the CV scanning rate (0.02 V s^{-1}). The diffusion coefficient of potassium ferricyanide ($D_R = 7.6 \times 10^{-6}$ cm^2 s^{-1})

Double-layer capacitance (C_{dl}) measurements were conducted by CV scanning from 0.36 to 0.48 V with different scan rates (20, 40, 60, 80 and 100 mV s^{-1}). Δj can be obtained through ja-jc, corresponding to the current density difference at the intermediate potential of the CV potential.

The electrochemical behavior was characterized by Electrochemical impedance spectroscopy (EIS) at open-circuit potential (frequency range: 0.1 Hz - 100 kHz). Long-term stability performance was quantified through chronoamperometry.

A constant current of 50 mA (200 mA cm^{-2}) was applied for 60 minutes to a two-electrode cell (working electrode area: 0.25 cm^2) to drive the oxygen evolution reaction (OER). The Faraday efficiency (FE) for oxygen production was calculated as the ratio of the experimentally measured gas volume (at standard temperature and pressure) to the theoretical volume derived from the total charge passed.

Supporting Figures

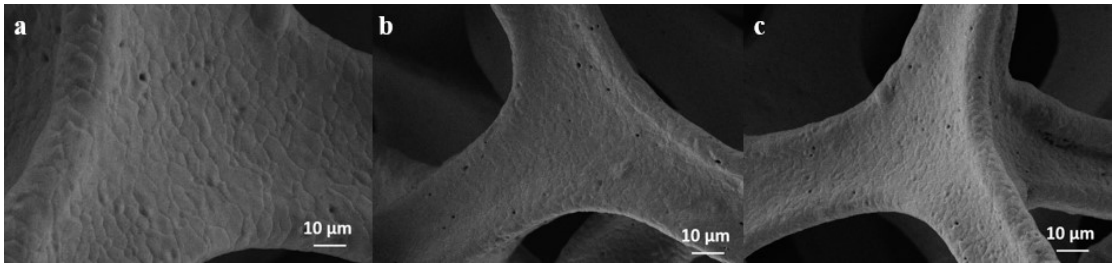

Fig. S1. SEM images of NF.

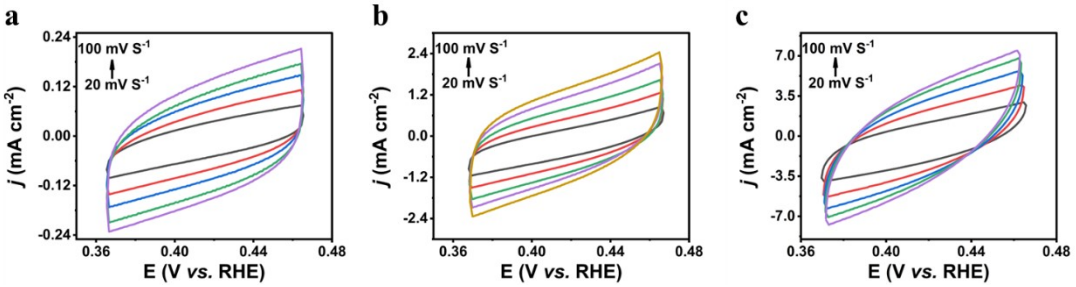

Fig. S2. CV curves at different scan rates of (a) Bare NF, (b) $Ni_{0.75}Fe_{0.15}Ce_{0.10}O_x$/NF and (c) N-$Ni_{0.75}Fe_{0.15}Ce_{0.10}P$/NF.

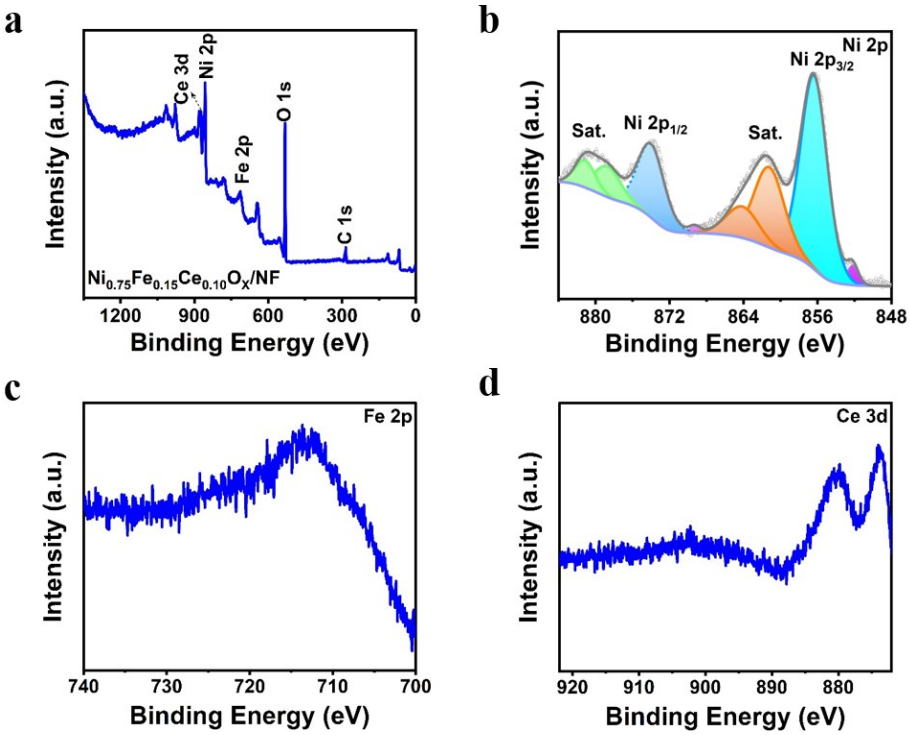

Fig. S3. (a) X-ray photoelectron spectroscopy (XPS) spectra of $Ni_{0.75}Fe_{0.15}Ce_{0.10}O_x$/NF; High-resolution XPS spectra of (b) Ni 2p, (c) Fe 2p and (d) Ce 3d in $Ni_{0.75}Fe_{0.15}Ce_{0.10}O_x$/NF.

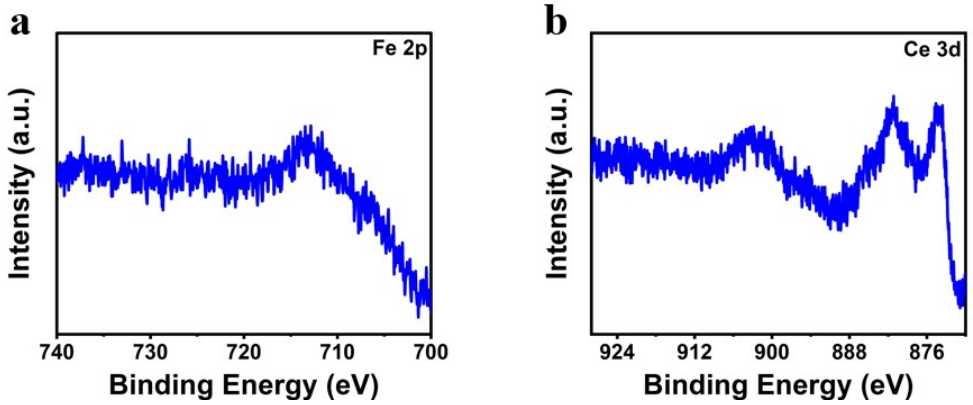

Fig. S4. High-resolution XPS spectra of (a) Fe 2p and (b) Ce 3d in N-$Ni_{0.75}Fe_{0.15}Ce_{0.10}P$/NF.

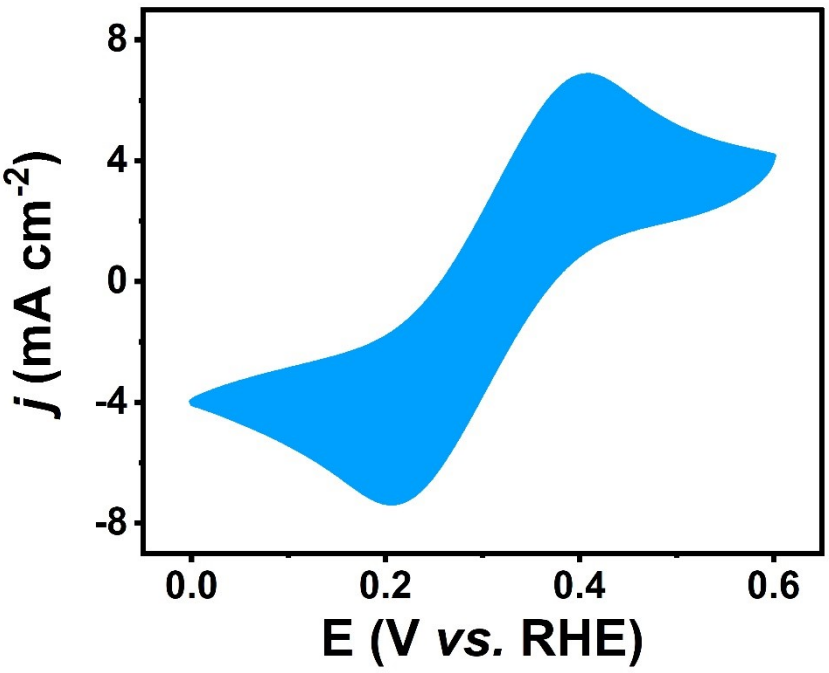

Fig. S5. CV curve recorded by NF in potassium ferriccyanide (5 mM) at a scanning rate of 50 mV s^{-1}.

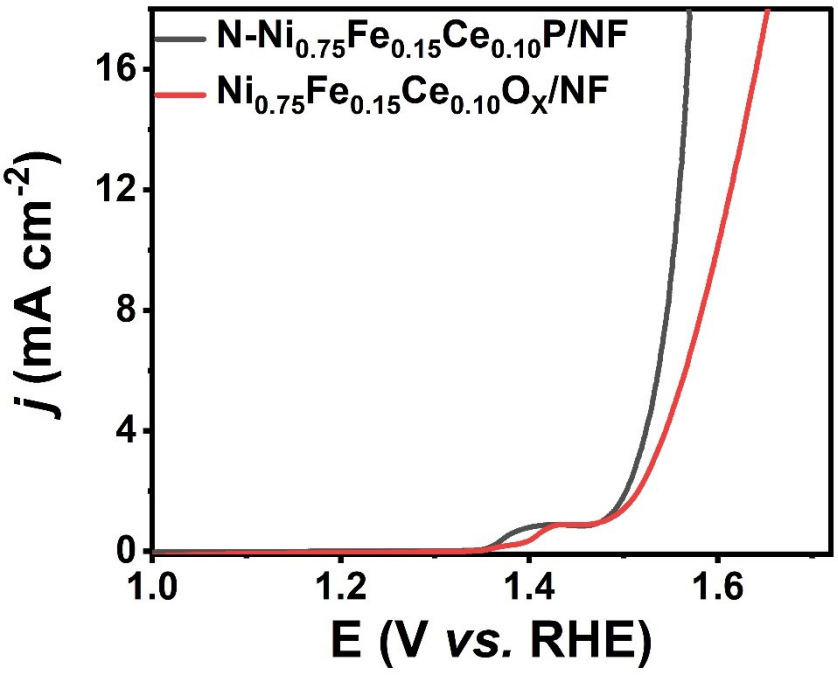

Fig. S6. Electrochemical surface area normalization OER polarization curves.

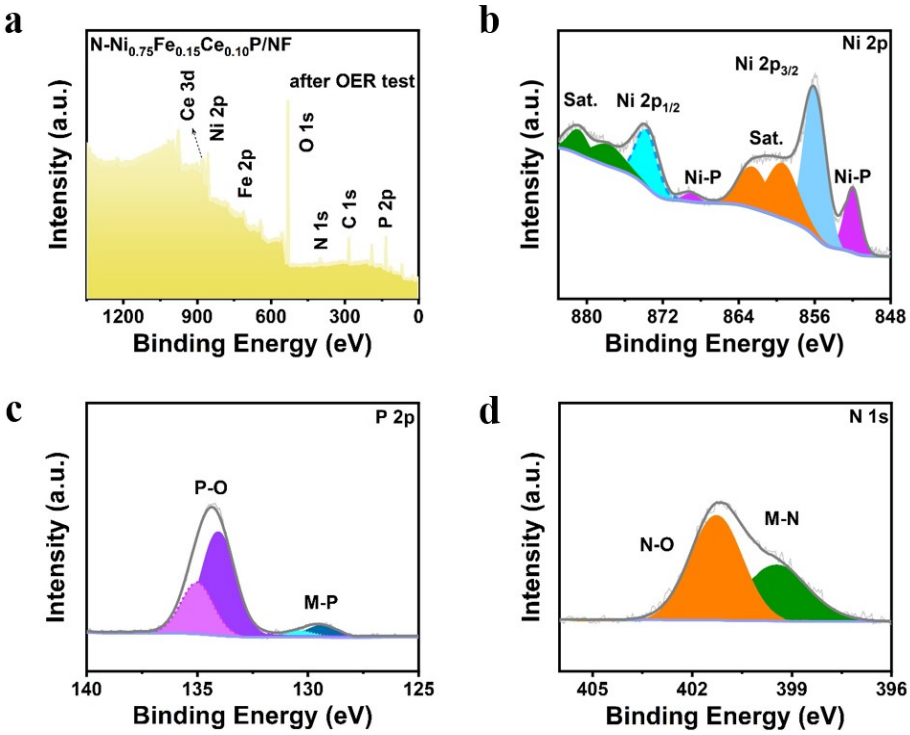

Fig. S7. (a) XPS survey spectrum of N-$Ni_{0.75}Fe_{0.15}Ce_{0.10}P$/NF after OER test; High-resolution XPS spectra of (b) Ni 2p, (c) P 2p and (d) N 1s in N-$Ni_{0.75}Fe_{0.15}Ce_{0.10}P$/NF after OER test.

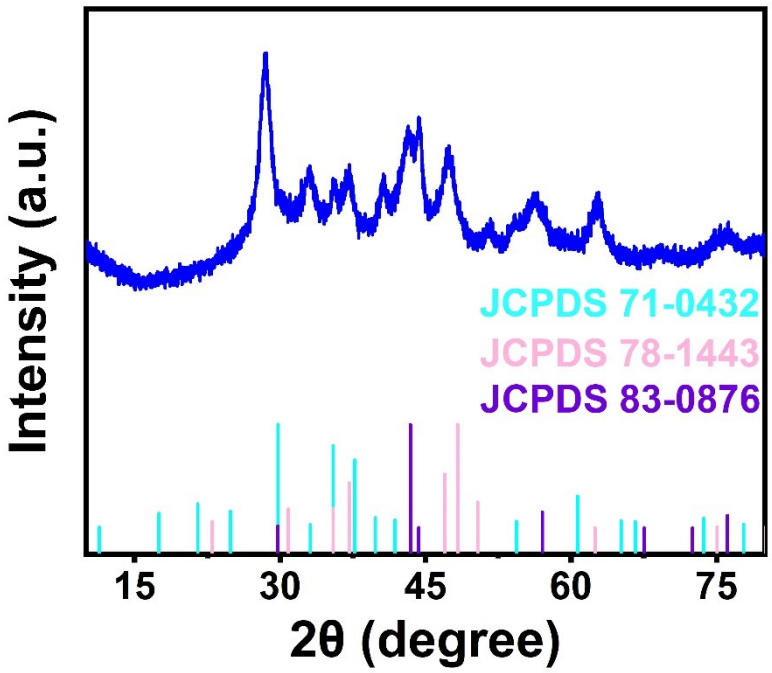

Fig. S8. XRD image of N-$Ni_{0.75}Fe_{0.15}Ce_{0.10}P$/NF after OER test

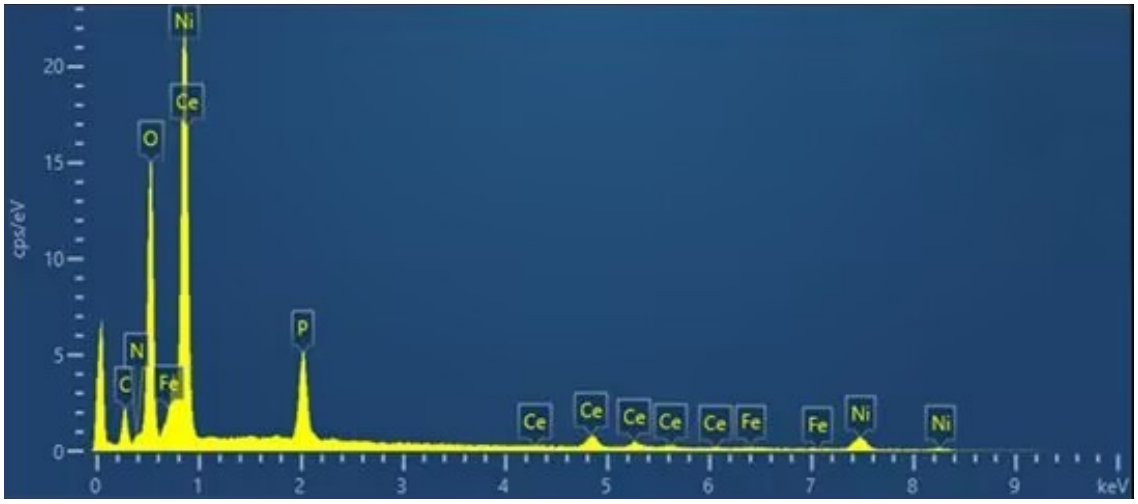

Fig. S9. EDX spectrum for N-$Ni_{0.75}Fe_{0.15}Ce_{0.10}P$/NF.

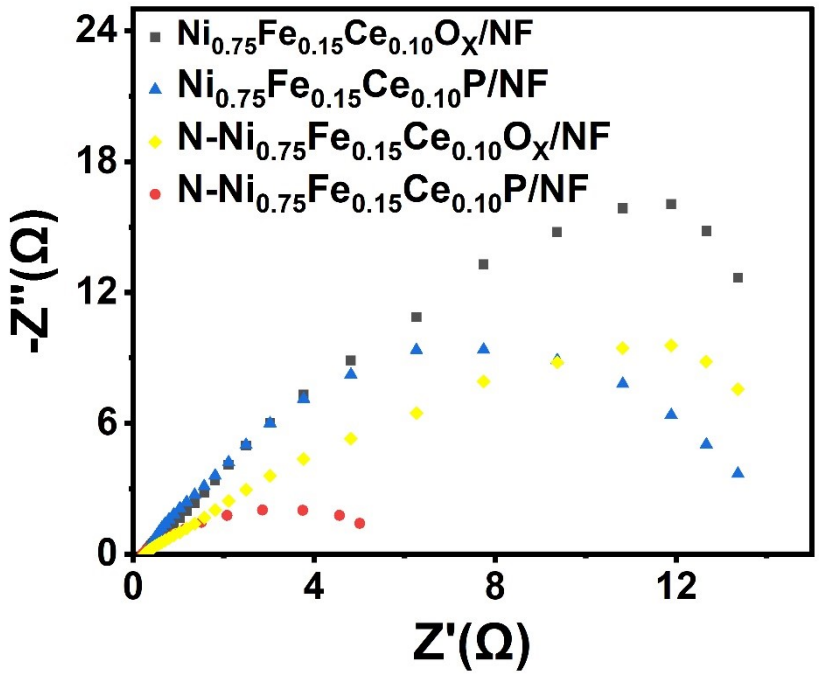

Fig. S10. Nyquist plots of different non-metallic element-doped materials obtained at open-circuit potential.

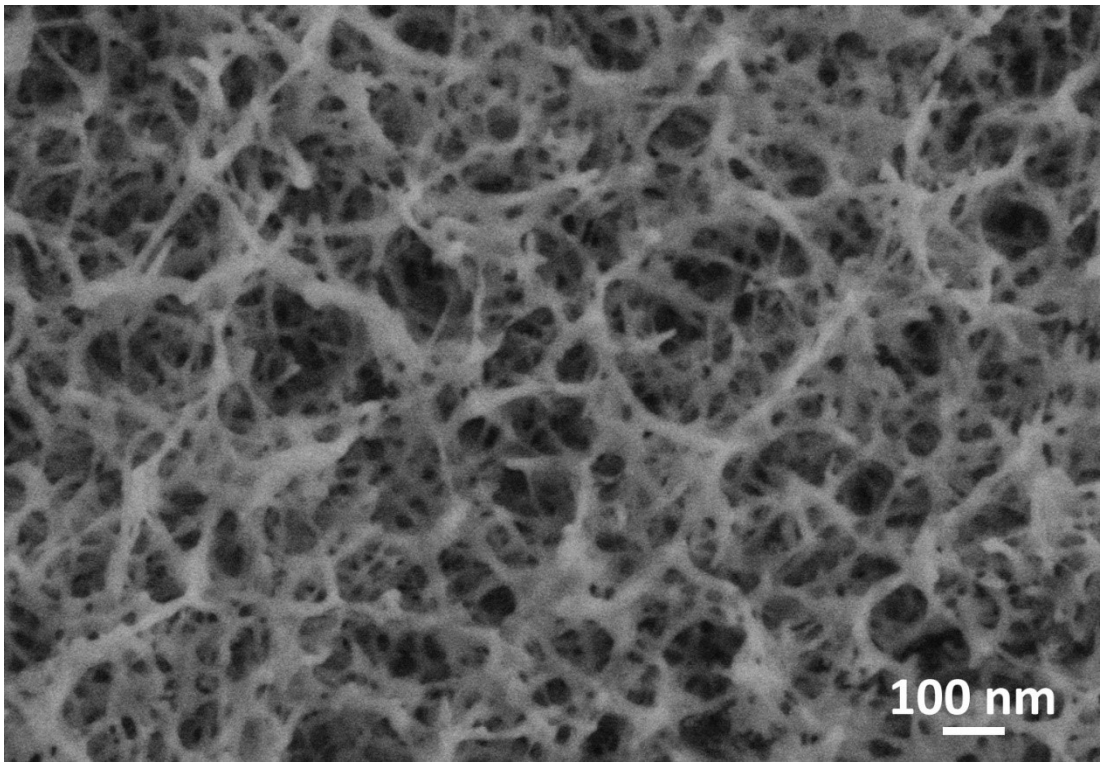

Fig. S11. SEM image of N-$Ni_{0.75}Fe_{0.15}Ce_{0.10}P$/NF after stability test.

Table S1. Comparison of OER performance of N-$Ni_{0.75}Fe_{0.15}Ce_{0.10}P$/NF and other Nickel-based catalyst in 1.0 M KOH

Catalyst	j (mA cm^{-2})	η (mV)	Ref.
N-$Ni_{0.75}Fe_{0.15}Ce_{0.10}P$/NF	50	244	This work
Ni_3N-CeO_2/NF	50	340	1
NiFeP/CoP	50	270	2
N, P-Ni/Mo-TEC@NF	50	317	3
Fe_xNi_y/CeO_2/NC	50	260	4
NiFe-LDH@NF	50	322	5
Ni_3Fe_1	50	346	6
N, Ce-NiCoP/NF	50	257	7

References

1 X. Ding, R. Jiang, J. Wu, M. Xing, Z. Qiao, X. Zeng, S. Wang and D. Cao, *Adv. Funct. Mater.*, 2023, 33, 2306786.

2 X. Jiang, Y. Li, M. He, L. Zhou, Q. Zheng, F. Xie, W. Jie and D. Lin, *Int. J. Hydrog. Energy*, 2019, 44, 19986-19994.

3 P. Zuo, X. Ji, J. Lu, Y. Chai, W. Jiao and R. Wang, *J Colloid Interface Sci*, 2023, 645, 895-905.

4 L. Chen, H. Jang, M. G. Kim, Q. Qin, X. Liu and J. Cho, *Inorg. Chem. Front.*, 2020, 7, 470-476.

5 L. Wang, D. Liu, Z. Zhang, Y. Li, J. Liu, Y. Yang, B. Xue and F. Li, *J. Alloys Compd.*, 2023, 934, 167846.

6 E. Chuluunbat, A. N. Nguyen, O. Omelianovych, A. Szaniel, L. L. Larina and H.-S. Choi, *Int. J. Hydrog. Energy*, 2024, 71, 102-109.

7 T. Zhao, G. Xu, B. Gong, J. Jiang and L. Zhang, *Nano Res.*, 2023, 17, 282-289.